Journal of Colloid and Interface Science 383 (2012) 198–207

Contents lists available at SciVerse ScienceDirect

Journal of Colloid and Interface Science

www.elsevier.com/locate/jcis

Onset of Marangoni convection for evaporating sessile droplets

Brendan D. MacDonald, C.A. Ward *

Thermodynamics and Kinetics Laboratory, Department of Mechanical and Industrial Engineering, University of Toronto, Toronto, Canada M5S 3G8

ARTICLE INFO

Article history:
Received 19 April 2012
Accepted 9 June 2012
Available online 27 June 2012

Keywords:
Evaporation
Marangoni instability
Sessile droplets

ABSTRACT

We have generated stability parameters using a linear stability analysis to predict the onset criteria for Marangoni convection in evaporating sessile droplets for two types of substrates, insulating and conducting. The stability problem was formulated with boundary conditions that allow for a temperature discontinuity at the liquid–vapour interface and the inclusion of an expression for the evaporation flux that considers this temperature discontinuity. We introduce no fitting coefficients; therefore, the stability parameters we generate contain only physical variables. The results indicate that spherical sessile droplets evaporating on insulating substrates are predicted to have a similar onset criteria with sessile droplets evaporating on conducting substrates. The onset prediction for sessile droplets evaporating on insulating substrates is found to be considerably different than the case of liquids evaporating from conical funnels constructed of insulating materials owing to the modification of the boundary condition from the geometrical shift and the corresponding retention of modes in the solution. A parametric analysis demonstrates how the input variables impact the stability of evaporating sessile droplets.

1. Introduction

The evaporation of sessile droplets is ubiquitous, with applications ranging from particle deposition and pattern formation [1–4], to biomedical [5,6], to thermal management in microelectronic devices [7]. Recently, an experimental investigation [8] demonstrated that Marangoni convection can play an important role in transporting thermal energy during the evaporation of sessile droplets. They demonstrated that for certain cases as much as 98% of the energy required for evaporation was transported along the liquid–vapour interface by Marangoni convection. An understanding of the onset criteria for Marangoni convection in sessile droplets would be beneficial for exploiting this phenomenon in applications.

Many researchers have investigated the Marangoni flow patterns in evaporating sessile droplets [1,9–12,2,13,14]. It has been argued that the direction and magnitude of the circulating flow within evaporating sessile droplets depends sensitively on the ratio of thermal conductivities of the liquid and substrate [2,13,14]. Despite the extensive investigations of the behaviour of Marangoni flow in evaporating sessile droplets, to the best of our knowledge, there have been no examinations of the onset criterion for the transition from quiescent evaporation to Marangoni convection.

The seminal investigation of the onset criteria for Marangoni convection was performed by Pearson [15]. The study was the first to demonstrate the role played by surface tension forces in initiating a cellular convection pattern, which had previously been attributed to buoyancy forces. The work has been studied experimentally for non-volatile liquids [16] and expanded upon theoretically by many other researchers, for example by Nield [17], who investigated the combined effect of surface tension and buoyancy. However, the theory developed by Pearson is not applicable to the evaporation of sessile droplets for two reasons, evaporation and geometry, which form the basis of this paper.

It has been demonstrated by several experimental investigations that the theory of Pearson [15] is not applicable to evaporating liquids [18–20]. A number of theoretical studies have also noted the inability of the theory to predict the onset of Marangoni convection for evaporating liquids and described the reasons [21,22]. As described in a recent article [22], the disparate predictions are likely due to the approximation of a temperature discontinuity at the interface in the opposite direction to that observed experimentally [23], and the complications associated with calculating an accurate value for the Biot number given the approximation.

The seminal theory of Pearson [15] was derived for a semi-infinite liquid sheet, a geometrical configuration that varies significantly from a sessile droplet. The semi-infinite liquid sheet enables the interface to be isolated from the boundary effects. The traditional mechanism for the instability is the development of a sufficiently large temperature gradient in the bulk liquid phase which disturbs the balance between surface tension and viscous forces at the interface. However, in the case of a sessile droplet, the interface is in contact with a bounding surface at the three-phase contact line; therefore, temperature gradients

* Corresponding author.
E-mail addresses: brendan.macdonald@utoronto.ca (B.D. MacDonald), charles.ward@utoronto.ca (C.A. Ward).

0021-9797/$ - see front matter © 2012 Elsevier Inc. All rights reserved.
http://dx.doi.org/10.1016/j.jcis.2012.06.046

in the bulk liquid phase would result in a tangential temperature gradient along the interface, which would immediately cause Marangoni convection to occur for any magnitude of temperature gradient (this would not be true exclusively in the case where the substrate material had the same conductivity as the bulk liquid phase). The seminal theory is therefore unable to predict the onset to Marangoni convection for evaporating sessile droplets and a stability analysis is required to consider the impact of a bounding wall in contact with the interface.

An analysis of liquids evaporating from conical funnels [24] demonstrated that the presence of a bounding wall results in stability parameters that are functions of the conditions at the interface instead of the temperature gradient in the bulk liquid phase. This stability analysis predicted that liquids evaporating from funnels constructed of insulating materials would be stable whereas liquids evaporating from funnels constructed of conducting materials could transition to Marangoni convection under certain conditions. The results were found to be in agreement with experimental observations [25,26,19]. The analysis of liquids evaporating from funnels differs from an analysis of evaporating sessile droplets since the location of the solid-liquid boundary is shifted, resulting in different boundary conditions.

In this paper we derive the stability parameters to predict the onset criterion for evaporating sessile droplets with an initially isothermal liquid phase. The stability problem was formulated with boundary conditions that allow for a temperature discontinuity at the liquid–vapour interface and the inclusion of an expression for the evaporation flux that considers this temperature discontinuity. The resulting stability parameters for evaporating sessile droplets contain only physical variables and no fitting coefficients. We demonstrate that the geometry has a significant impact on the results of the stability predictions since the results differ from those found for the analysis of liquids evaporating from conical funnels [24]. In contrast to the funnel investigation, the stability of sessile droplets evaporating on insulating and conducting substrates is found to be similar, and both cases are expected to transition to Marangoni convection. We show that the differing predictions between the funnel and sessile droplet analyses is caused by the modes retained in the solution as a result of the modified boundary conditions from the angular shift of the bounding surface. A parametric analysis is performed based on the experiments of Ristenpart et al. [2] to demonstrate how the input variables impact the stability predictions and give insight as to the applicability of assumptions used to describe evaporating sessile droplets.

2. Problem definition

We perform the investigation for an evaporating spherical sessile droplet with an interface at $r = r_I$ that is bounded at a polar angle of $\pi/2$ by a substrate, as shown in Fig. 1. The system is axisymmetric about the $\phi = 0$ centreline. The surrounding fluid is the vapour phase of the liquid and has a temperature at a boundary far from the interface of T_∞. Here the polar angle is given by ϕ as θ is used to denote the temperature perturbation. We assume the liquid–vapour interface is not deformable, which is a good approximation excepting cases with high evaporation rates and thin liquid layers. For the linear stability analysis the velocity and temperature in the liquid phase and the temperature in the vapour phase are perturbed and analyzed. The temperature of the vapour phase is included to ensure a balance of energy, and the effect of velocity in the vapour phase is assumed to be negligible. These details are consistent with the previous investigation for the funnel geometry [24], so that we can compare the results and assess the difference induced by the geometrical modification.

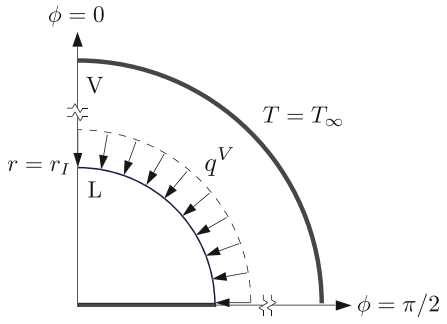

Fig. 1. Schematic of spherical sessile droplet geometry.

As noted in Section 1, for a spherical sessile droplet geometry in contact with the bounding surface, temperature gradients in the liquid phase would also result in tangential temperature gradients along the interface, which would cause Marangoni convection. Therefore, in order to have an initially stable state to perturb from, it is a requirement that the liquid phase be isothermal. This assumption is consistent with the previous funnel geometry analysis and the experimental observations [25,26,19] that were used as the basis for the assumption in that study [24]. The initial state therefore requires that the energy necessary for evaporation be provided by conduction through the vapour phase (shown in Fig. 1 as q^V).

The analysis is performed for two different types of substrates, insulating and conducting. This will enable comparison of the results from the sessile droplet analysis to those from the funnel geometry.

3. Governing equations and boundary conditions

The liquid phase is assumed to be incompressible and buoyancy effects to be negligible, so the governing equations are mass, momentum, and energy conservation as follows

$$\nabla \cdot \mathbf{U} = 0, \tag{1}$$

$$\frac{\partial \mathbf{U}}{\partial t} + \mathbf{U} \cdot \nabla \mathbf{U} = -\frac{1}{\rho}\nabla P + \nu \nabla^2 \mathbf{U}, \tag{2}$$

$$\frac{\partial T^L}{\partial t} + \mathbf{U} \cdot \nabla T^L = \alpha \nabla^2 T^L, \tag{3}$$

where $\mathbf{U}$ is the velocity in the liquid phase, t is time, ρ is the density of the liquid, P is the pressure, ν is the kinematic viscosity, T^L is the temperature of the liquid phase, and α is the thermal diffusivity in the liquid.

As noted above, the effect of velocity in the vapour phase is assumed to be negligible, so we require only the energy conservation equation for the vapour phase, which reduces to

$$\frac{\partial T^V}{\partial t} = \alpha^V \nabla^2 T^V, \tag{4}$$

where T^V is the temperature of the vapour phase, and α^V is the thermal diffusivity in the vapour phase.

At $\phi = \pi/2$ there is a rigid side wall so the boundary conditions on the velocity are

$$U_r = U_\phi = 0. \tag{5}$$

At the bounding wall, we list the energy boundary conditions individually for each substrate type. For the insulating case

$$-\frac{1}{r}\frac{\partial T^L}{\partial \phi}\bigg|_{\phi=\frac{\pi}{2}} = 0. \tag{6}$$

For the conducting substrate, we require an energy balance in the liquid phase between the substrate and evaporation at the liquid–vapour interface, so that instead of Eq. (6) the condition is

$$\left(\int_0^{r_l} -\frac{\partial T^L}{\partial \phi}\sin\phi dr\right)_{\left(\phi=\frac{\pi}{2}\right)} = \left(\int_0^{\frac{\pi}{2}} \frac{\partial T^L}{\partial r} r^2 \sin\phi d\phi\right)_{(r=r_l)}. \tag{7}$$

At $\phi = 0$ we have an axisymmetric boundary, which yields

$$\frac{\partial U_r}{\partial \phi} = 0, \tag{8}$$

$$U_\phi = \frac{\partial U_\phi}{\partial \phi} = 0, \tag{9}$$

$$\frac{\partial T^L}{\partial \phi} = 0, \tag{10}$$

$$\frac{\partial T^V}{\partial \phi} = 0. \tag{11}$$

At $r \to \infty$ the vapour phase temperature satisfies

$$T^V = T_\infty. \tag{12}$$

At $r = r_l$ we have evaporation at a free surface, which is a discontinuous liquid–vapour interface. Therefore, we generate the boundary conditions using discontinuity conditions for the balance laws as follows

$$\rho U_r = j_{ev}, \tag{13}$$

$$\nu\rho\left(\frac{1}{r_l}\frac{\partial U_r}{\partial \phi} + \frac{\partial U_\phi}{\partial r} - \frac{U_\phi}{r_l}\right) = \frac{\gamma_T}{r_l}\frac{\partial T^L}{\partial \phi}, \tag{14}$$

$$\kappa^V \frac{\partial T^V}{\partial r} - \kappa^L \frac{\partial T^L}{\partial r} - \left(\frac{c_\sigma U_\phi}{r_l}\frac{\partial T^L}{\partial \phi}\right) = j_{ev}\left[h^V\left(T^V\right) - h^L\left(T^L\right)\right], \tag{15}$$

where j_{ev} is the evaporation flux at the interface, γ_T is the change of surface tension with respect to temperature, κ is the thermal conductivity (with V and L superscripts denoting the liquid and vapour phases), c_σ is the surface thermal capacity [25], $h^V\left(T^V\right)$ is the enthalpy of the vapour, and $h^L\left(T^L\right)$ is the enthalpy of the liquid. It is noted in Eq. (14) that the vapour phase is not included. Since for many fluids the viscosity of the vapour phase is negligible compared to the viscosity of the liquid phase, the vapour phase velocity would not contribute to Eq. (14), and so the vapour phase velocity can be considered negligible, as was noted above.

4. Initial steady-state solution

Initially, we assume that the liquid is evaporating with no Marangoni convection. As noted above, we assume that initially we have an isothermal liquid phase whereby the energy required for evaporation is provided by conduction through the vapour phase, and the vapour phase temperature gradient normal to the interface is uniform along the interface. We also assume that the initial evaporation rate is low enough so that the effect of flow through the liquid phase is negligible, and the initial velocities are zero. Thus we have

$$\mathbf{U}_{ini} = \mathbf{0}, \tag{16}$$

$$P_{ini} = P_0, \tag{17}$$

$$T^L_{ini} = T_0, \tag{18}$$

$$T^V_{ini} = T^V_{ini}(r), \tag{19}$$

where the *ini* subscript denotes the initial state, and a 0 subscript or superscript denotes the initial, unperturbed value of the variable.

With the low flow rate assumption and dependence only in the radial direction, the initial temperature distribution in the vapour phase is governed by a simplified form of Eq. (4) as follows

$$\frac{1}{r^2}\frac{\partial}{\partial r}\left(r^2\frac{\partial T^V_{ini}}{\partial r}\right) = 0. \tag{20}$$

When the assumptions listed above are applied to the boundary condition, Eq. (12), we have

$$T^V_{ini}(r \to \infty) = T_\infty, \tag{21}$$

$$\left.\frac{\partial T^V_{ini}}{\partial r}\right|_{r=r_l} = \beta, \tag{22}$$

where β denotes the uniform vapour phase temperature gradient normal to the interface. We note that β can be determined in the initial state with the following relation to the evaporation flux from Eq. (15)

$$\beta = \frac{j^0_{ev}\left(h^V_0 - h^L_0\right)}{\kappa^V}. \tag{23}$$

The solution of Eq. (20) with Eqs. (22) and (21) is

$$T^V_{ini}(r) = T_\infty + \beta\left(-\frac{r_l^2}{r}\right). \tag{24}$$

This initial steady-state solution will provide the basis for perturbations in the linear stability analysis.

5. Perturbation equations

Based on the initial state, we introduce the following perturbations

$$\mathbf{U}(r,\phi,t) = \mathbf{u}(r,\phi,t), \tag{25}$$

$$P(r,\phi,t) = P_0 + p(r,\phi,t), \tag{26}$$

$$T^L(r,\phi,t) = T_0 + \theta^L(r,\phi,t), \tag{27}$$

$$T^V(r,\phi,t) = T_\infty + \beta\left(-\frac{r_l^2}{r}\right) + \theta^V(r,\phi,t), \tag{28}$$

and we reiterate that the velocity perturbation and pressure perturbation are for the liquid phase only, so no superscript is included on them.

Since the evaporation flux and enthalpy of vapourization depend on the liquid and vapour temperatures, a perturbed form of these parameters is required. They can be expanded as

$$j_{ev} = j^0_{ev} + \frac{\partial j_{ev}}{\partial T^L}\theta^L + \frac{\partial j_{ev}}{\partial T^V}\theta^V, \tag{29}$$

$$\left[h^V\left(T^V\right) - h^L\left(T^L\right)\right] = \left(h^V_0 - h^L_0\right) - c^L_p\theta^L + c^V_p\theta^V, \tag{30}$$

where c_p is the specific heat capacity. It can be seen from Eq. (29) that an expression for the evaporation flux is required, which will allow for the derivative to be taken with respect to both liquid and vapour temperatures. The requirements on such an expression are that it be capable of considering a temperature discontinuity at the liquid–vapour interface and that it have no fitting coefficients.

An expression for the evaporation flux, j_{ev}, such as that derived from statistical rate theory [27], could be used.

We introduce the following non-dimensionalizations

$$r = r^* r_I, \tag{31}$$

$$t = \frac{t^* r_I^2}{\nu}, \tag{32}$$

$$U_r = \frac{U_r^* \alpha}{r_I}, \tag{33}$$

$$U_\phi = \frac{U_\phi^* \alpha}{r_I}, \tag{34}$$

$$P = \frac{P^* \rho \nu \alpha}{r_I^2}, \tag{35}$$

$$T^L = T^{L*} \beta r_I, \tag{36}$$

$$T^V = T^{V*} \beta r_I, \tag{37}$$

When the perturbations and scalings are substituted into the conservation equations, Eqs. (1)–(4), the following linearized equations result (the asterisk is dropped from the variables and the analysis is non-dimensional from here onward)

$$\mathbf{\nabla} \cdot \mathbf{u} = 0, \tag{38}$$

$$\frac{\partial \mathbf{u}}{\partial t} = -\mathbf{\nabla} p + \nabla^2 \mathbf{u}, \tag{39}$$

$$\mathrm{Pr} \frac{\partial \theta^L}{\partial t} - \nabla^2 \theta^L = 0, \tag{40}$$

$$\frac{\nu}{\alpha^V} \frac{\partial \theta^V}{\partial t} - \nabla^2 \theta^V = 0, \tag{41}$$

where Pr is the Prandtl number in the liquid phase (ν/α). The pressure term can be eliminated by taking the curl of Eq. (39) twice yielding

$$\frac{\partial}{\partial t} \nabla^2 \mathbf{u} - \nabla^4 \mathbf{u} = \mathbf{0}, \tag{42}$$

We now have a linearized and non-dimensional set of governing equations, Eqs. (38), (42), and (40), and the linear stability analysis can be performed. The linearized and non-dimensional boundary conditions are derived in the following section.

6. Marginal stability

For this analysis we adopt the traditional assumption that the marginally stable state of a system corresponds to neutral stability and exceeding this criteria generates an instability. The marginally stable state of the system can be described if we assign the following form to the perturbations

$$u_r = u_{rs}(r, \phi) \exp(\sigma t), \tag{43}$$

$$u_\phi = u_{\phi s}(r, \phi) \exp(\sigma t), \tag{44}$$

$$\theta^L = \theta_s^L(r, \phi) \exp(\sigma t), \tag{45}$$

$$\theta^V = \theta_s^V(r, \phi) \exp(\sigma t). \tag{46}$$

The governing equations, Eqs. (38), (42), (40), and (41) become, respectively,

$$\mathbf{\nabla} \cdot \mathbf{u}_s = 0, \tag{47}$$

$$\sigma \nabla^2 \mathbf{u}_s - \nabla^4 \mathbf{u}_s = \mathbf{0}, \tag{48}$$

$$\mathrm{Pr} \sigma \theta_s^L - \nabla^2 \theta_s^L = 0, \tag{49}$$

$$\frac{\nu}{\alpha^V} \sigma \theta_s^V - \nabla^2 \theta_s^V = 0. \tag{50}$$

We assume the exchange of stabilities is valid, so that σ is real, the marginally stable states are characterized by $\sigma = 0$, and Eqs. (48)–(50) become

$$\nabla^4 \mathbf{u}_s = \mathbf{0}, \tag{51}$$

$$\nabla^2 \theta_s^L = 0, \tag{52}$$

$$\nabla^2 \theta_s^V = 0. \tag{53}$$

The perturbations, Eqs. (25), (29), (30), and stability equations, Eqs. (43), (46), can now be substituted into the boundary conditions from Section 3. At $\phi = \pi/2$, we substitute into Eq. (5) yielding

$$u_{\phi s} = 0. \tag{54}$$

It is noted that slip is allowed along the boundary wall in the perturbed velocity.

For the insulating substrate, at $\phi = \pi/2$, we substitute into Eq. (6) yielding

$$-\frac{1}{r} \frac{\partial \theta_s^L}{\partial \phi}\bigg|_{\phi=\frac{\pi}{2}} = 0. \tag{55}$$

For the conducting substrate, we substitute into Eq. (7) yielding

$$\left(\int_0^1 -\frac{\partial \theta_s^L}{\partial \phi} \sin\phi dr \right)_{\left(\phi=\frac{\pi}{2}\right)} = \left(\int_0^{\frac{\pi}{2}} \frac{\partial \theta_s^L}{\partial r} r^2 \sin\phi d\phi \right)_{(r=1)}. \tag{56}$$

At $\phi = 0$, Eqs. (8)–(11) become

$$\frac{\partial u_{rs}}{\partial \phi} = 0, \tag{57}$$

$$u_{\phi s} = \frac{\partial u_{\phi s}}{\partial \phi} = 0, \tag{58}$$

$$\frac{\partial \theta_s^L}{\partial \phi} = 0, \tag{59}$$

$$\frac{\partial \theta_s^V}{\partial \phi} = 0. \tag{60}$$

For $r \to \infty$, Eq. (12) becomes

$$\theta_s^V = 0. \tag{61}$$

At $r = 1$, Eqs. (13)–(15) become

$$u_{rs} = \frac{r_I^2 \beta}{\rho \alpha} \left(\frac{\partial j_{ev}}{\partial T^L} \theta_s^L + \frac{\partial j_{ev}}{\partial T^V} \theta_s^V \right), \tag{62}$$

$$\frac{\partial^2 u_{rs}}{\partial r^2} - \frac{\partial^2 u_{rs}}{\partial \phi^2} + 2 \frac{\partial u_{rs}}{\partial r} - \cot\phi \frac{\partial u_{rs}}{\partial \phi} - 2 u_{rs} = -\frac{\gamma_T r_I^2 \beta}{\rho \nu \alpha} \left(\frac{\partial^2 \theta_s^L}{\partial \phi^2} + \cot\phi \frac{\partial \theta_s^L}{\partial \phi} \right), \tag{63}$$

$$\frac{\kappa^V}{\kappa^L} \frac{\partial \theta_s^V}{\partial r} + \frac{r_I}{\kappa^L} \left(-\frac{\partial j_{ev}}{\partial T^V} \left(h_0^V - h_0^L \right) - j_{ev}^0 c_p^V \right) \theta_s^V = \frac{\partial \theta_s^L}{\partial r} + \frac{r_I}{\kappa^L} \left(\frac{\partial j_{ev}}{\partial T^L} \left(h_0^V - h_0^L \right) - j_{ev}^0 c_p^L \right) \theta_s^L, \tag{64}$$

We have simplified Eq. (63) to eliminate the dependence on $u_{\phi s}$ by first differentiating by ϕ then substituting in the continuity equation, Eq. (47), and finally substituting the undifferentiated initial form to yield the form shown above. With this simplification we require a solution for only u_{rs} in the stability analysis. For convenience we define the dimensionless groupings from these equations as follows

$$\xi_{CL} = \frac{r_I^2 \beta}{\rho \alpha} \frac{\partial j_{ev}}{\partial T^L}, \tag{65}$$

$$\xi_{CV} = \frac{r_I^2 \beta}{\rho \alpha} \frac{\partial j_{ev}}{\partial T^V}, \tag{66}$$

$$\xi_M = \left(-\frac{\gamma_T r_I^2 \beta}{\rho \nu \alpha} \right), \tag{67}$$

$$K = \frac{\kappa^V}{\kappa^L}, \tag{68}$$

$$\xi_{TV} = \frac{r_I}{\kappa^L} \left(-\frac{\partial j_{ev}}{\partial T^V} \left(h_0^V - h_0^L \right) - j_{ev}^0 c_p^V \right), \tag{69}$$

$$\xi_{TL} = \frac{r_I}{\kappa^L} \left(\frac{\partial j_{ev}}{\partial T^L} \left(h_0^V - h_0^L \right) - j_{ev}^0 c_p^L \right), \tag{70}$$

and it is noted that each of these parameters contain only properties or measurable variables, thus making them physical parameters. The conditions at $r = 1$ are rewritten

$$u_{rs} = \xi_{CL} \theta_s^L + \xi_{CV} \theta_s^V, \tag{71}$$

$$\frac{\partial^2 u_{rs}}{\partial r^2} - \frac{\partial^2 u_{rs}}{\partial \phi^2} + 2 \frac{\partial u_{rs}}{\partial r} - \cot \phi \frac{\partial u_{rs}}{\partial \phi} - 2 u_{rs} = \xi_M \left(\frac{\partial^2 \theta_s^L}{\partial \phi^2} + \cot \phi \frac{\partial \theta_s^L}{\partial \phi} \right), \tag{72}$$

$$K \frac{\partial \theta_s^V}{\partial r} + \xi_{TV} \theta_s^V = \frac{\partial \theta_s^L}{\partial r} + \xi_{TL} \theta_s^L. \tag{73}$$

The ξ_M term in Eq. (72) is traditionally called the Marangoni number. We have defined ξ_M in Eq. (67), so it represents the Marangoni number for a spherical system with an initially isothermal liquid phase and a temperature gradient in the vapour phase. The stability criterion will be developed by substituting the solutions for the velocity and temperature perturbations into Eq. (72) and solving for ξ_M.

The change-of-phase process at the liquid–vapour interface allows a non-zero value for the radial velocity in Eq. (71). The ξ_{CL} and ξ_{CV} terms relate a temperature change (in the liquid and vapour phase respectively) to the radial velocity at the interface of an evaporating fluid.

The liquid and vapour phase temperatures are coupled because we include the contributions from both phases in the energy balance of Eq. (73). The physical interpretation of the ξ_{TV} and ξ_{TL} terms is evident with an analogy to the Biot number, since their placement in Eq. (73) indicates they have replaced the Biot number and have the same role. Therefore, the ξ_{TV} term represents the ratio of the resistance to conduction through the vapour phase and the resistance to the evaporation flux at the interface. Likewise, the ξ_{TL} term represents the ratio of the resistance to conduction through the liquid phase and the resistance to the evaporation flux at the interface. These terms have a crucial role in the stability of the system, as is demonstrated by the generation of the stability parameters in Eqs. (94) and (104), which are listed below.

It is noted that the boundary conditions, Eqs. (54)–(61) and Eqs. (71)–(73)do not comprise a complete set and so the governing equations, Eqs. (51)–(53), are not closed. All of the boundary conditions have been implemented for the physical problems being investigated in this study, with Eqs. (55) and (56) being of particular importance. If the stability analysis proceeds in a general form using only the boundary conditions listed above, it is found that the coefficients are cancelled from the stability parameters derived in the following sections, so no additional boundary conditions are required to adequately describe the stability.

It would be possible to close the system with respect to the temperatures if there were an additional boundary condition predicting the magnitude of the temperature discontinuity between the interfacial liquid and vapour phase temperatures. At present, to the best of our knowledge, no such expression exists. A temperature discontinuity is included in Eq. (73), which ensures a balance of energy and also enables any magnitude of temperature discontinuity to be applied. If a heat flux is given, it is possible to use statistical rate theory to predict one of the interfacial temperatures given the other one. However this requires an additional input and therefore does not close the system. If the theory were to be developed, it is possible to use a kinetic expression, similar to the statistical rate theory expression for the evaporation flux, to describe the energy flux at the interface. If such an expression were to be developed it would possible to have the capability to predict the magnitude of the temperature discontinuity at an evaporating interface.

7. Insulating substrate

We perform an analysis for spherical sessile droplets evaporating on insulating substrates, using the equations listed above.

7.1. Liquid phase temperature

The general solution to Laplace's equation, Eq. (52), for the liquid phase temperature perturbation is given as

$$\theta_s^L(r, \phi) = \sum_{n=0}^{\infty} \left(A_n r^n + B_n r^{-n-1} \right) P_n(\cos \phi), \tag{74}$$

where $P_n(\cos \phi)$ are the Legendre polynomials.

In order for the solution to be bounded at the origin, $B_n = 0$ for all n. We substitute Eq. (74) into Eq. (55) yielding

$$-\frac{1}{r} \frac{\partial \theta_s^L}{\partial \phi}\bigg|_{\phi=\frac{\pi}{2}} = -\sum_{n=0}^{\infty} (n+1) A_n r^{n-1} P_{n+1}(0) = 0. \tag{75}$$

Therefore, $A_n = 0$ for all odd values of n. We emphasize here the significance of this boundary condition. For the funnel geometry with the insulating bounding wall located at an angle of $\pi/4$ all of the terms for $n > 0$ were eliminated [24]. However, for the sessile droplet geometry, all of the even modes are retained, so they provide contributions to the solution and generate a significantly different prediction for the onset of Marangoni convection.

The boundary condition from Eq. (59) is satisfied

$$\frac{\partial \theta_s^L}{\partial \phi}\bigg|_{\phi=0} = 0. \tag{76}$$

The expression for θ_s^L is thus

$$\theta_s^L(r, \phi) = \sum_{n=0}^{\infty} (A_n r^n) P_n(\cos \phi), \tag{77}$$

for only even values of n. This expression will be used in Section 7.4 to derive the stability criterion.

7.2. Vapour phase temperature

The general solution for the temperature in the vapour phase is

$$\theta_s^V(r,\phi)=\sum_{n=0}^{\infty}\left(C_n r^n + D_n r^{-n-1}\right)P_n(\cos\phi). \tag{78}$$

The vapour phase does not include the origin, so the D_n coefficients remain, and instead $C_n = 0$ for all n, from the boundary condition at $r \to \infty$, Eq. (61).

We substitute Eq. (78) into Eq. (73) and find

$$\sum_{n=0}^{\infty}\left(D_n(\xi_{TV}-K(n+1))\right)P_n(\cos\phi) = \sum_{n=0}^{\infty}\left(A_n(n+\xi_{TL})\right)P_n(\cos\phi), \tag{79}$$

for even values of n. Therefore $D_n = A_n(n+\xi_{TL})/(\xi_{TV}-K(n+1))$. The boundary condition from Eq. (60) is satisfied

$$\left.\frac{\partial\theta_s^V}{\partial\phi}\right|_{\phi=0} = 0. \tag{80}$$

The expression for θ_s^V is

$$\theta_s^V(r,\phi)=\sum_{n=0}^{\infty}\frac{A_n(n+\xi_{TL})}{(\xi_{TV}-K(n+1))}r^{-n-1}P_n(\cos\phi), \tag{81}$$

for even values of n. Similar to the expression for θ_s^L, this expression will be used in Section 7.4 in order to derive the stability criterion.

7.3. Liquid phase radial velocity

The general solution to the spherical biharmonic equation, Eq. (51), is given as [28]

$$u_{rs}(r,\phi)=\sum_{n=0}^{\infty}\left(E_n r^{n+2}+F_n r^n + G_n r^{1-n} + H_n r^{-1-n}\right)P_n(\cos\phi). \tag{82}$$

In order for the the solution to be bounded at the origin $G_n = 0$ for $n > 1$ and $H_n = 0$ for all n. The boundary condition from Eq. (57) is satisfied

$$\left.\frac{\partial u_{rs}}{\partial\phi}\right|_{\phi=0} = 0. \tag{83}$$

We substitute Eq. (82) into Eq. (71) and find

$$G_0 + G_1\cos\phi + \sum_{n=0}^{\infty}(E_n+F_n)P_n(\cos\phi) = \sum_{n=0}^{\infty}A_n\left(\xi_{CL}+\frac{\xi_{CV}(n+\xi_{TL})}{\xi_{TV}-K(n+1)}\right)P_n(\cos\phi). \tag{84}$$

There are no additional boundary conditions to limit which of the coefficients in Eq. (84) are used in the expression for u_{rs}

$$u_{rs}(r,\phi)=G_0 r + G_1\cos\phi + \sum_{n=0}^{\infty}\left(E_n r^{n+2}+F_n r^n\right)P_n(\cos\phi), \tag{85}$$

so the stability problem is solved considering all of the coefficients and the resulting solutions are analyzed with respect to their physical validity.

7.4. Examination of the coefficients

In order to derive the stability criterion Eq. (72) is rearranged and the s subscript is added to distinguish the result of the stability analysis from the physical definition of ξ_M given above in Eq. (67)

$$\xi_{Ms} = \frac{\left(\frac{\partial^2 u_{rs}}{\partial r^2} - \frac{\partial^2 u_{rs}}{\partial\phi^2} + 2\frac{\partial u_{rs}}{\partial r} - \cot\phi\frac{\partial u_{rs}}{\partial\phi} - 2u_{rs}\right)}{\left(\frac{\partial^2\theta_s^L}{\partial\phi^2}+\cot\phi\frac{\partial\theta_s^L}{\partial\phi}\right)}. \tag{86}$$

Substituting in the solutions for θ_s^L Eq. (77), θ_s^V Eq. (81), and u_{rs} Eq. (85) yields

$$\xi_{Ms} = \frac{1}{A_n}\left(\frac{-2E_n(n+1)(n+2)-2F_n\left(n^2+n-1\right)}{n(n+1)}\right), \tag{87}$$

for even values of n, and $n > 0$.

The E_n and F_n coefficients in Eq. (87) are investigated individually. There are two possible cases, Eq. (84) can either be solved for E_n with F_n set equal to zero (Case E), or for F_n with E_n set equal to zero (Case F). Utilizing combinations of these terms would result in a description of the stability parameter with ambiguous constants, which would have to be eliminated, so only these two cases are considered. Case E yields

$$\xi_{Ms}^E = -\left(\frac{2(n+2)}{n}\right)\left(\xi_{CL}+\frac{\xi_{CV}(n+\xi_{TL})}{\xi_{TV}-K(n+1)}\right), \tag{88}$$

and Case F yields

$$\xi_{Ms}^F = -\left(\frac{2\left(n^2+n-1\right)}{n(n+1)}\right)\left(\xi_{CL}+\frac{\xi_{CV}(n+\xi_{TL})}{\xi_{TV}-K(n+1)}\right), \tag{89}$$

for all even values of n greater than zero. The form given in Eq. (89) is a multiple of Eq. (88), so we analyze only Eq. (88) since the multiplier is larger for all even values of n greater than zero, and therefore the parameter is larger and corresponds to the least stable case.

7.5. Stability parameter for an insulating substrate

To examine the stability we equate the result from the perturbation analysis, Eq. (88), and the physical definition of ξ_M from Eq. (67)

$$-\left(\frac{2(n+2)}{n}\right)\left(\xi_{CL}+\frac{\xi_{CV}(n+\xi_{TL})}{\xi_{TV}-K(n+1)}\right) = \xi_M. \tag{90}$$

Substituting in Eqs. (65)–(67) and rearranging terms yields

$$-\frac{r_l^2\beta}{\rho\alpha}\left(\frac{2(n+2)}{n}\right)\left[\left.\frac{\partial j_{ev}}{\partial T^L}\right|_I+\left.\frac{\partial j_{ev}}{\partial T^V}\right|_I\left(\frac{n+\xi_{TL}}{\xi_{TV}-K(n+1)}\right)\right] = -\frac{\gamma_T r_l^2\beta}{\rho\nu\alpha}. \tag{91}$$

The ξ_{TL} and ξ_{TV} terms were not substituted for, since no simplification results from the substitution. The terms common to both sides of the equation can be cancelled

$$-\left(\frac{2(n+2)}{n}\right)\left[\left.\frac{\partial j_{ev}}{\partial T^L}\right|_I+\left.\frac{\partial j_{ev}}{\partial T^V}\right|_I\left(\frac{n+\xi_{TL}}{\xi_{TV}-K(n+1)}\right)\right] = -\frac{\gamma_T}{\nu}. \tag{92}$$

We see from Eq. (92) that an expression has now been generated that relates the evaporation properties of the fluid to the ratio between the surface tension forces and viscous forces. In order to generate a stability parameter which is dimensionless we rearrange Eq. (92) as follows

$$\frac{\nu}{\gamma_T}\left[\left.\frac{\partial j_{ev}}{\partial T^L}\right|_I+\left.\frac{\partial j_{ev}}{\partial T^V}\right|_I\left(\frac{n+\xi_{TL}}{\xi_{TV}-K(n+1)}\right)\right] = \left(\frac{n}{2(n+2)}\right). \tag{93}$$

We define the stability parameter, χ_s^{ID} (the ID superscript refers to the case of a sessile droplet on an insulating substrate), as the left hand side of Eq. (93)

$$\chi_s^{ID} = \frac{\nu}{\gamma_T}\left[\left.\frac{\partial j_{ev}}{\partial T^L}\right|_I+\left.\frac{\partial j_{ev}}{\partial T^V}\right|_I\left(\frac{n+\xi_{TL}}{\xi_{TV}-K(n+1)}\right)\right], \tag{94}$$

for even values of n greater than zero. From the right hand side of Eq. (93) the onset criteria for this parameter occurs at a value of

$$\left(\frac{n}{2(n+2)}\right). \tag{95}$$

The value of n corresponds to the solutions from spherical harmonics and it can thus be determined from the number of convection cells present in an evaporating sessile droplet. Selection of a value for n is demonstrated in Section 9 for the parametric analysis of a sessile droplet evaporating on a conducting substrate.

We emphasize that χ_s^{ID} is comprised entirely of physical variables that are either properties or parameters that can be measured, so this expression could be compared directly with experimental observations. In contrast to the conventional stability investigations for non-volatile fluids and semi-infinite systems, the stability parameter does not depend on temperature gradients, since β was cancelled in Eq. (91). Therefore, the expression for the stability parameter is instead a function of the conditions at the interface. Also the importance of including the vapour phase thermal contributions in the interfacial energy balance, Eq. (73), is noted since the vapour phase contributions are present in the stability parameter, particularly the K term, which is the ratio of thermal conductivity of the vapour and liquid phases.

There presently exist no experiments for evaporating sessile droplets which we can compare to the stability parameter, χ_s^{ID}, in order to produce a quantitative corroboration.

In contrast to the stability parameter generated in Eq. (94), the case of liquids evaporating from funnels constructed of insulating materials was found to be stable regardless of the evaporation rate [19,24]. This indicates that the location of the funnel wall at $\phi = \pi/4$ serves to suppress the modes that would generate an instability in the sessile droplet case. Therefore, the geometry plays a critical role in the generation of Marangoni convection for evaporating liquids with spherical interfaces bounded by insulating materials.

8. Conducting substrate

In this section we develop an expression to predict the onset of Marangoni convection for spherical sessile droplets evaporating on conducting substrates.

8.1. Liquid phase temperature

Similar to the analysis above, the general solution to Laplace's equation is Eq. (74), and in order for the solution to be bounded at the origin, $B_n = 0$ for all n. Substituting into Eq. (56), both integrals are found to be equivalent, so Eq. (56) is satisfied. The boundary condition from Eq. (59) is also satisfied

$$\left.\frac{\partial \theta_s^L}{\partial \phi}\right|_{\phi=0} = 0. \tag{96}$$

Therefore, the expression for θ_s^L is

$$\theta_s^L(r,\phi) = \sum_{n=0}^{\infty}(A_n r^n)P_n(\cos\phi). \tag{97}$$

This expression will be used in Section 8.4 to derive the stability criterion.

The solution for the liquid phase temperature perturbation, Eq. (97), allows us to comment on the direction of Marangoni flow in evaporating sessile droplets that has been discussed by [2,13,14] as noted in Section 1. For this analysis, the energy balance in the liquid phase along the substrate boundary and the liquid–vapour interface, given by Eq. (56), determines the tangential temperature gradient along the interface, and thus, the direction of Marangoni flow. The solution of Eq. (97) indicates that the liquid phase temperature perturbation is multiplied by a constant, A_n. This constant can either have a positive or negative value. If the constant is positive (Case 1), the substrate will provide heat to the liquid, thus generating a warmer temperature at the three phase contact line and inducing Marangoni flow towards the apex of the droplet. Conversely, if the constant is negative (Case 2), the substrate will remove heat from the liquid, thus generating a cooler temperature at the three phase contact line and inducing Marangoni flow from the apex towards the three phase contact line. Therefore, this analysis allows for the possibility of flow in either direction, and the direction is dictated by the sign of the A_n constant for the liquid phase temperature perturbation solution. These two cases are illustrated in Fig. 2.

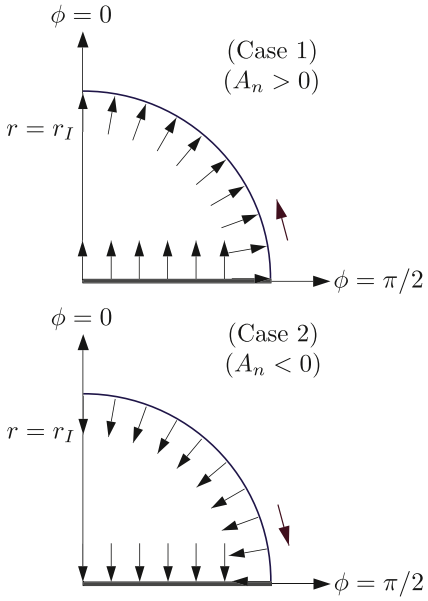

Fig. 2. Schematic of the two possible directions of Marangoni flow based on the sign of the A_n coefficient.

8.2. Vapour phase temperature

Similar to the analysis above, the general solution to Laplace's equation is Eq. (78), and in order for the solution to be bounded at $r \to \infty$ according to Eq. (61), $C_n = 0$ for all n. Substituting into Eq. (73) yields

$$\sum_{n=0}^{\infty}(D_n(\xi_{TV} - K(n+1)))P_n(\cos\phi) = \sum_{n=0}^{\infty}(A_n(n+\xi_{TL}))P_n(\cos\phi). \tag{98}$$

Therefore $D_n = A_n(n+\xi_{TL})/(\xi_{TV} - K(n+1))$. The boundary condition from Eq. (60) is satisfied

$$\left.\frac{\partial \theta_s^V}{\partial \phi}\right|_{\phi=0} = 0. \tag{99}$$

The expression for θ_s^V is

$$\theta_s^V(r,\phi) = \sum_{n=0}^{\infty}\frac{A_n(n+\xi_{TL})}{(\xi_{TV} - K(n+1))}r^{-n-1}P_n(\cos\phi). \tag{100}$$

Similar to the expression for θ_s^L, this expression will be used in Section 8.4 in order to derive the stability criterion.

8.3. Liquid phase radial velocity

Similar to the analysis for an insulating substrate, the general solution to the spherical biharmonic equation is Eq. (82), and for the solution to be bounded at the origin $G_n = 0$ for $n > 1$ and $H_n = 0$ for all n. The boundary condition from Eq. (57) is satisfied

$$\left.\frac{\partial u_{rs}}{\partial \phi}\right|_{\phi=0} = 0. \tag{101}$$

We substitute Eq. (82) into Eq. (71) and find

$$G_0 + G_1 \cos\phi + \sum_{n=0}^{\infty}(E_n + F_n)P_n(\cos\phi) = \sum_{n=0}^{\infty} A_n\left(\xi_{CL} + \frac{\xi_{CV}(n+\xi_{TL})}{\xi_{TV} - K(n+1)}\right)P_n(\cos\phi). \tag{102}$$

There are no additional boundary conditions to limit which of the coefficients in Eq. (102) are used in the expression for u_{rs}

$$u_{rs}(r,\phi) = G_0 r + G_1 \cos\phi + \sum_{n=0}^{\infty}(E_n r^{n+2} + F_n r^n)P_n(\cos\phi), \tag{103}$$

so the stability problem is solved considering all of the coefficients and the resulting solutions are analyzed with respect to their physical validity.

8.4. Stability parameter for a conducting substrate

At this point we recognize that the solutions for θ_s^L (Eq. (97)), θ_s^V (Eq. (100)), and u_{rs} (Eq. (103)) are the same as those derived for the insulating substrate above in Section 7, with the only difference being that for the conducting case the modes are not restricted to only even values. Therefore, the derivation of the stability parameter proceeds in the same fashion as above and, χ_s^{CD}, (the CD superscript refers to the case of a sessile droplet on a conducting substrate) is found to be

$$\chi_s^{CD} = \frac{v}{\gamma_T}\left[\left.\frac{\partial j_{ev}}{\partial T^L}\right|_I + \left.\frac{\partial j_{ev}}{\partial T^V}\right|_I\left(\frac{n+\xi_{TL}}{\xi_{TV} - K(n+1)}\right)\right], \tag{104}$$

with the onset criteria at a value of

$$\left(\frac{n}{2(n+2)}\right). \tag{105}$$

As noted above, the value of n is from spherical harmonics and is related to the number of convection cells present in an evaporating sessile droplet. We demonstrate selection of a value for n in Section 9 for the parametric analysis.

Similar to χ_s^{ID}, χ_s^{CD} is comprised entirely of physical variables that are either properties or parameters that can be measured, so this expression could be compared directly with experimental observations if any presently existed. As noted above, in order to ensure that no fitting parameters are present in the onset predictions, the derivatives of evaporation flux with respect to the interfacial liquid and vapour temperatures in Eq. (104) should be calculated with an expression for evaporation flux that is free of fitting parameters, such as the expression generated by statistical rate theory [27]. In contrast to the case of insulating substrates analyzed above, for both sessile droplet and funnel geometry [24], the stability parameter was the same for boundaries constructed of conducting materials.

We note that the stability parameters for insulating, χ_s^{ID}, and conducting, χ_s^{CD}, substrates are similar. The only difference being the retention of the even values of n for the insulating case, but all values of n for the conducting case. Therefore, this analysis predicts that insulating and conducting substrates have similar stability predictions.

9. Parametric analysis of the stability parameter

In this section we perform a parametric analysis of the stability parameter for sessile droplets evaporating on conducting substrates, χ_s^{CD}, in order to understand how the input variables impact the stability and also to demonstrate how the stability parameter may be applied to predict the onset of Marangoni convection for a physical system. As the base case for the analysis we select an evaporating sessile droplet of ethanol examined in the experimental investigation of Ristenpart et al. [2].

The streamlines drawn in Fig. 4 of reference [2] illustrate the presence of one large circulation cell for Marangoni flow in the evaporating sessile droplet. This indicates that the $n = 1$ mode is the least stable mode since this pattern corresponds to the $n = 1$ solution for the spherical harmonics. Therefore we substitute $n = 1$ into Eq. (104) yielding the stability parameter for this analysis

$$\chi_s^{CD(n=1)} = \frac{v}{\gamma_T}\left[\left.\frac{\partial j_{ev}}{\partial T^L}\right|_I + \left.\frac{\partial j_{ev}}{\partial T^V}\right|_I\left(\frac{1+\xi_{TL}}{\xi_{TV} - 2K}\right)\right], \tag{106}$$

and an onset criteria value from Eq. (105) equal to 1/6 (or 0.167).

Examination of Eq. (106) reveals that the stability parameter is a function of the evaporation flux, the interfacial liquid and vapour temperatures, the vapour phase pressure of the system, and the radius of the spherical droplet. Based on the information provided by Ristenpart et al. [2] we can approximate the values of these parameters as 1 g/m^{2}s, 24.5 °C, 25 °C, 7064 Pa, and 1 mm respectively, and assume the droplet is spherical. We selected a temperature discontinuity value of 0.5 °C because there are no interfacial temperature measurements reported for this experiment and this value is consistent with the experimental observations of another investigation where the interfacial liquid and vapour phase temperatures were measured for an evaporating sessile droplet of water [8].

The only remaining terms in Eq. (106) are the derivatives of the evaporation flux with respect to the interfacial liquid and vapour phase temperatures. As noted above in Section 5 we require an expression for the evaporation flux that considers both interfacial liquid and vapour phase temperatures separately (allowing for a temperature discontinuity at the interface), and has no fitting coefficients. For this purpose we select the statistical rate theory expression for the evaporation flux [27], which has been included in Appendix A.

The methodology for the parametric analysis is to analyze each parameter individually while the others are held constant. We list the results for the evaporation flux, the interfacial liquid and vapour temperatures, and the radius of the spherical droplet but not the vapour phase pressure since it is found to have a negligible effect on the stability.

9.1. Effect of interfacial vapour phase temperature

The result of varying T_I^V while holding the other variables fixed is plotted in Fig. 3. It can be seen that as T_I^V is decreased from the base value of 25 °C, the system becomes unstable. Since T_I^L is fixed in this case, as T_I^V is decreased, it approaches the value of T_I^L (24.5 °C); thus, the temperature discontinuity at the interface ($\Delta T_I = T_I^V - T_I^L$) is decreasing. Therefore, the analysis indicates that as T_I^V decreases the system becomes less stable, or alternatively, as the temperature discontinuity decreases the system becomes less stable.

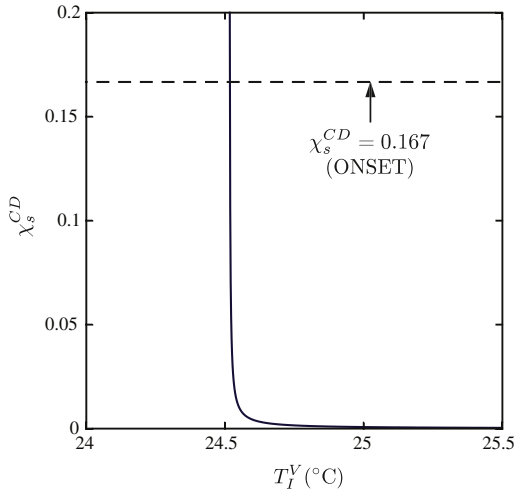

Fig. 3. Stability parameter, χ_s^{CD}, with $n = 1$ for evaporating ethanol, is plotted versus T_I^V for T_I^L fixed at 24.5 °C, j_{ev} at 1 g/m^{2}s, and r_I at 1 mm.

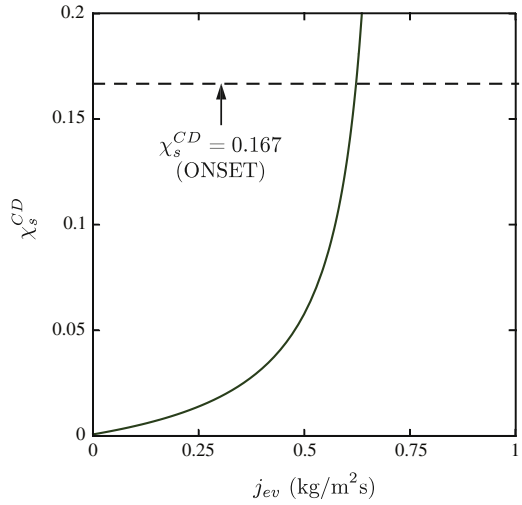

Fig. 5. Stability parameter, χ_s^{CD}, with $n = 1$ for evaporating ethanol, is plotted versus j_{ev} for T_I^V fixed at 25 °C, T_I^L at 24.5 °C, and r_I at 1 mm.

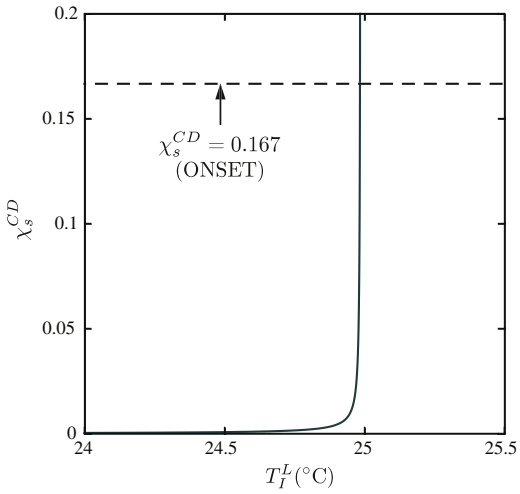

Fig. 4. Stability parameter, χ_s^{CD}, with $n = 1$ for evaporating ethanol, is plotted versus T_I^L for T_I^V fixed at 25 °C, j_{ev} at 1 g/m^{2}s, and r_I at 1 mm.

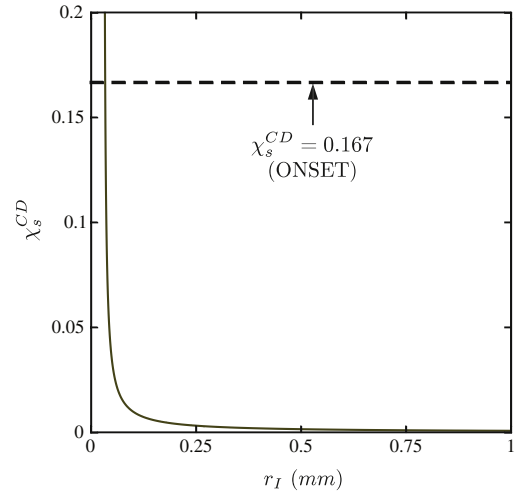

Fig. 6. Stability parameter, χ_s^{CD}, with $n = 1$ for evaporating ethanol, is plotted versus r_I for T_I^V fixed at 25 °C, T_I^L at 24.5 °C, and j_{ev} at 1 g/m^{2}s.

9.2. Effect of interfacial liquid phase temperature

The result of varying T_I^L is plotted in Fig. 4. It can be seen that as T_I^L is increased from the base value of 24.5 °C, the system becomes unstable. Similar to the T_I^V analysis it is interesting to observe the effect of decreasing the temperature discontinuity. Since T_I^V is fixed in this case, as T_I^L is increased, it approaches the value of T_I^V (25 °C); thus, the temperature discontinuity at the interface is decreasing. Therefore, the analysis indicates that as T_I^L increases the system becomes less stable, or alternatively and consistent with the T_I^V case, as the temperature discontinuity decreases the system becomes less stable.

We note that this analysis predicts the onset to Marangoni convection to occur for a temperature discontinuity value of approximately 0.02 °C, with the other parameters fixed at the base values listed above. This indicates that a small but non-zero value for the temperature discontinuity is required for an instability, which differs from the assumption of zero temperature discontinuity that is traditionally assumed when analyzing evaporating sessile droplets with Marangoni convection present.

9.3. Effect of evaporation flux

The result of varying j_{ev} is plotted in Fig. 5. It can be seen that as j_{ev} is increased from the base value of 1 g/m^{2}s, the system becomes unstable. We also observe from Fig. 5 that the evaporation flux expected to yield an instability with the other variables fixed at their base values is approximately three orders of magnitude higher than the base value approximated from the reported experiment. This indicates that the onset to Marangoni instability is affected only by large changes in the evaporation flux and is more sensitive to changes in the other variables.

9.4. Effect of the spherical droplet radius

The result of varying r_I is plotted in Fig. 6. It can be seen that as r_I is decreased from the base value of 1 mm, the system becomes unstable. This indicates that smaller evaporating sessile droplets are less stable than larger ones.

10. Conclusion

A linear stability analysis has been performed and a stability parameter was generated to characterize the stability of sessile droplets evaporating on insulating substrates, χ_s^{ID}, and conducting substrates, χ_s^{CD}. The values for the onset to Marangoni convection were also determined. The results indicate that spherical sessile droplets evaporating on insulating substrates are predicted to have similar stability predictions with sessile droplets evaporating on conducting substrates.

A comparison of the stability parameter for sessile droplets evaporating on insulating substrates with the results from an analysis of liquids evaporating from funnels constructed of insulating materials [24] demonstrated that the onset predictions are considerably different owing to the modification of the boundary condition from the geometrical shift and the corresponding retention of modes in the solution. The analysis for the funnel case predicted no transition to Marangoni convection whereas the analysis for the sessile droplet case generated a stability parameter which indicates that a transition to Marangoni convection is predicted.

We demonstrated that the solution for the liquid phase temperature perturbation from the analysis of a sessile droplet evaporating on a conducting substrate allows for the direction of Marangoni flow either away from or towards the three phase contact line. Therefore, it is possible to predict the onset criteria for sessile droplets with Marangoni flow in either direction.

A parametric analysis was performed for the stability parameter for sessile droplets evaporating on conducting substrates. The analysis demonstrated how the stability predictions can be generated without any fitting parameters when statistical rate theory is used to determine the derivatives of evaporation flux with respect to the liquid and vapour phase temperatures. The result from the parametric analysis is that smaller interfacial temperature discontinuities, higher evaporation rates, and smaller droplets correspond to less stable systems.

Acknowledgments

We would like to acknowledge the support of the Canadian and European Space Agencies and the Natural Sciences and Engineering Research Council of Canada.

Appendix A. Statistical rate theory expression for evaporation flux

The evaporation flux is given by Ward and Fang [27]

$$j_{ev} = 2mK_e \sinh\left(\frac{\Delta s_{lv}}{k_b}\right), \tag{A.1}$$

where

$$K_e = \frac{\eta P_s(T_I^L)}{\sqrt{2\pi m k_b T_I^L}},$$

$$\eta = exp\left[\frac{v_f(T_I^L)}{k_b T_I^L}\left(P_e^L - P_s(T_I^L)\right)\right],$$

$$\frac{\Delta s_{lv}}{k_b} = \ln\left[\left(\frac{T_I^V}{T_I^L}\right)^4 \frac{P_s(T_I^L)}{P^V}\right] + \ln\left[\frac{q_{vib}(T_I^V)}{q_{vib}(T_I^L)}\right] + 4\left(1 - \frac{T_I^V}{T_I^L}\right) + \left(\frac{1}{T_I^V} - \frac{1}{T_I^L}\right)\sum_{l=1}^{3n-6}\left[\frac{\theta_l}{2} + \frac{\theta_l}{e^{\theta_l/T_I^V - 1}}\right] + \frac{v_f(T_I^L)}{k_b T_I^L}\left[P^V + \frac{2\gamma^{LV}(T)}{r_I} - P_s(T_I^L)\right], \theta_l = \frac{\hbar\omega_l}{k_b},$$

$$q_{vib}(T) = \prod_{l=1}^{3n-6} \frac{e^{-\theta_l/2T}}{1 - e^{-\theta_l/T}},$$

and P_e^L must satisfy

$$P_e^L - \frac{2\gamma^{LV}(T)}{r_I} = \eta P_s(T_I^L),$$

where k_b is the Boltzmann constant, n is the number of atoms in the molecule, $\hbar$ is the reduced Planck constant, m is the mass of a molecule undergoing evaporation, ω_l is a molecular phonon, v_f is the specific volume of the liquid at saturation, γ^{LV} is the surface tension at the liquid–vapour interface, $P_s(T_I^L)$ is the saturation pressure, and P_e^L is the liquid pressure that would exist at equilibrium. The values of the properties for ethanol are listed in [29] along with an examination of the use of the statistical rate theory expression for evaporation flux with ethanol as the evaporating fluid.

References

[1] R.D. Deegan, O. Bakajin, T.F. Dupont, G. Huber, S.R. Nagel, T.A. Witten, Nature 389 (1997) 827–829.
[2] W.D. Ristenpart, P.G. Kim, C. Domingues, J. Wan, H.A. Stone, Phys. Rev. Lett. 99 (2007) 243502.
[3] P.J. Yunker, T. Still, M.A. Lohr, A.G. Yodh, Nature 476 (2011) 308–311.
[4] G. Berteloot, A. Hoang, A. Daerr, H.P. Kavehpour, F. Lequeux, L. Limat, J. Colloid Interface Sci. 370 (2012) 155–161.
[5] T.A. Yakhno, O.A. Sedova, A.G. Sanin, A.S. Pelyushenko, Tech. Phys. 48 (2003) 399–403.
[6] V. Dugas, J. Broutin, E. Souteyrand, Langmuir 21 (2005) 9130–9136.
[7] J. Kim, S.Y.S.U. Choi, Int. J. Heat Mass Transfer 47 (2004) 3307–3315.
[8] H. Ghasemi, C.A. Ward, Phys. Rev. Lett. 105 (2010) 136102.
[9] R.D. Deegan, Phys. Rev. E 61 (2000) 475–485.
[10] R.D. Deegan, O. Bakajin, T.F. Dupont, G. Huber, S.R. Nagel, T.A. Witten, Phys. Rev. E 62 (2000) 756–765.
[11] H. Hu, R.G. Larson, Langmuir 21 (2005) 3972–3980.
[12] F. Girard, M. Antoni, S. Faure, A. Steinchen, Langmuir 22 (2006) 11085–11091.
[13] G.J. Dunn, S.K. Wilson, B.R. Duffy, S. David, K. Sefiane, J. Fluid Mech. 623 (2009) 329–351.
[14] X. Xu, J. Luo, D. Guo, Langmuir 26 (2010) 1918–1922.
[15] J.R.A. Pearson, J. Fluid Mech. 4 (1958) 489–500.
[16] M.F. Schatz, S.J. VanHook, W.D. McCormick, J.B. Swift, H.L. Swinney, Phys. Rev. Lett. 75 (1995) 1938–1941.
[17] D.A. Nield, J. Fluid Mech. 19 (1964) 341–352.
[18] A.-T. Chai, N. Zhang, Exp. Heat Transfer 11 (1998) 187–205.
[19] I. Thompson, F. Duan, C.A. Ward, Phys. Rev. E 80 (2009) 056308.
[20] X. Song, D.S. Nobes, Exp. Therm. Fluid Sci. 35 (2011) 910–919.
[21] R. Liu, Q.-S. Liu, W.-R. Hu, Chin. Phys. Lett 22 (2005) 402–404.
[22] K.S. Das, B.D. MacDonald, C.A. Ward, Phys. Rev. E 81 (2010) 036318.
[23] G. Fang, C.A. Ward, Phys. Rev. E 59 (1999) 417–428.
[24] B.D. MacDonald, C.A. Ward, Phys. Rev. E 84 (2011) 046319.
[25] F. Duan, C.A. Ward, Phys. Rev. E 72 (2005) 056302.
[26] F. Duan, C.A. Ward, Phys. Rev. E 72 (2005) 056304.
[27] C.A. Ward, G. Fang, Phys. Rev. E 59 (1999) 429–440.
[28] A.D. Polyanin, Handbook of Linear Partial Differential Equations for Engineers and Scientists, Chapman & Hall/CRC, 2002.
[29] A.H. Persad, C.A. Ward, J. Phys. Chem. B 114 (2010) 6107–6116.